Materials and Design 31 (2010) 2916–2924

Contents lists available at ScienceDirect

Materials and Design

journal homepage: www.elsevier.com/locate/matdes

Geometry, mechanical properties and mounting of perforated plates for ballistic application

Sebastian Balos [a,*], Vencislav Grabulov [b], Leposava Sidjanin [a], Mladen Pantic [c], Igor Radisavljevic [c]

[a] University of Novi Sad, Faculty of Technical Sciences, Department of Production Engineering, Trg Dositeja Obradovica 6, 21000 Novi Sad, Serbia
[b] Institute for Materials Testing, Bulevar Vojvode Misica 43, 11000 Belgrade, Serbia
[c] Military Technical Institute, Ratka Resanovica 1, 11132 Belgrade, Serbia

ARTICLE INFO

Article history:
Received 28 August 2009
Accepted 15 December 2009
Available online 21 December 2009

Keywords:
A. Ferrous metals and alloys
E. Impact and ballistics
H. Failure analysis

ABSTRACT

In this paper, the ballistic resistance of perforated plates made of different types of steel, mounting and geometry was investigated. Different types of steel in various heat treatment conditions were tested. Target mounting was also varied: rigid, oblique and hanging. Furthermore, four different perforated plate geometries were tested: two plate thicknesses and two hole diameters. Their behaviour was tested using impact from firing 12.7 mm M-8 API ammunition at eleven perforated plate samples. These samples were placed by means of a steel frame over a 13 mm RHA plate, at two distances. Damaged area on targets was correlated to ballistic resistance of the whole armour to find the optimal perforated plate. It was found that perforated plates, in optimized case offer a frequent fracture of the penetrating core in up to five parts. This debris is unable to penetrate the basic plate, offering mass effectiveness of the whole armour model of 1.76 and the mass effectiveness of the perforated plate of 5.91.

1. Introduction

Applique add – on armour has always been a very attractive mean od improving passive protection of armoured vehicles. However, one of the main concerns about this type of protection is its weight, which might overstress the vehicles automotive components causing a significant loss of mobility and reliability. Therefore, applique armour types should have a higher mass efficiency than basic steel or aluminium alloy armour that forms the structure of the vehicle. As vehicles are often subjected to automatic weapons fire, where multiple projectiles are fired towards a limited area of armour, multi-hit protection needs to be provided. This problem has been noticed especially when brittle materials are used such as ceramics, which are still among the most widely used applique armour types [1,2]. On the other hand, brittle behaviour has been noticed on homogenous metallic armour (steel and aluminium alloys) as well, even if the ductility of these materials is higher than that of ceramics. Therefore, in [3] some cases have shown that 8 cm^2 aluminium alloy and steel plates were fractured in brittle manner after the impact by 7.62 mm AP projectiles. In a large-scale plates mounted as applique armour on an actual vehicle, these cracks might have serious consequences on multi-hit resistance. In this respect, perforated plates may offer a potentially more effective solution due to a higher ductility and a possibility of crack propagation from impact point to the nearest hole, leaving a larger portion of the armour intact in comparison to ceramics where the whole tile is destroyed [4–7].

Perforated plates induce bending stresses in the projectile penetrating core. As the core is made usually from high hardness steel, its ductility is also low, which when impact bending stresses are present might cause core fracture. This way, a significant drop of penetration is achieved, allowing a relatively thin basic armour to stop the debris. This core defeating mechanism has been thoroughly explained in [8].

In this paper, an attempt was made to investigate the influence of geometry (plate thickness, hole size, distance between holes) and mounting (stiff, oblique, hanging) of perforated plates as well as mechanical properties (strength, ductility) of the materials used for this application. A special attention is paid to the application of commercial steels as a way to use readily available off-the-shelf materials, useful when specialized armour steels are unavailable or in short supply. Such materials were previously considered for ballistic application by Edwards and Matthewson [9], who used tool steel in different heat treatment conditions. Borvik et al. [10] used five different high-strength steels as improvised armour, as an alternative to rolled homogenous armour (RHA). In contrast to [9,10], this paper may be understood as a "guide" to researchers for further optimization of different influential parameters of unhomogenous armour in form of a perforated plate. Authors are unaware of any paper or other publication in the open literature which address ballistic resistance of perforated plates.

* Corresponding author. Tel.: +381 214852339; fax: +381 454495.
E-mail address: sebab@uns.ns.ac.yu (S. Balos).

0261-3069/$ - see front matter © 2009 Elsevier Ltd. All rights reserved.
doi:10.1016/j.matdes.2009.12.031

The present work was carried out as a part of a continuing program at the University of Novi Sad, in collaboration with the Military Technical Institute – Belgrade to study and develop different types of ballistic protection systems for the defence industry.

Table 1
Chemical composition of 50CrV4 and Hardox 450.

	C	Si	Mn	Cr	Ni	P	S	V	Fe
50CrV4	0.55	0.36	0.82	0.99	0.20	0.033	0.013	0.13	Balance
Hardox 450	0.22	0.69	1.62	0.80	0.36	0.020	0.005	0.02	Balance

Table 2
Mechanical properties of tested materials.

	50CrV4 tempered at 170 °C	50CrV4 tempered at 450 °C	Hardox 450
Hardness BHN (kgf/mm^2)	598 ± 5	465 ± 4	445 ± 3
Ultimate tensile strength (MPa)	1885 ± 10	1470 ± 14	1450 ± 8
Yield strength (MPa)	1845 ± 15	1410 ± 13	1255 ± 7
Elongation (%)	3 ± 1	6 ± 1	11 ± 2
Contraction in radial direction (%)	14 ± 2	21 ± 3	45 ± 5
Impact strength (J)	5 ± 2	14 ± 2	60 ± 3

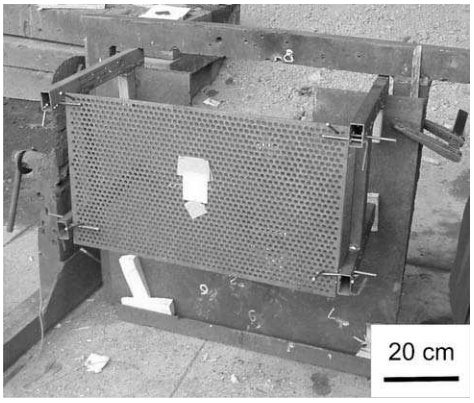

Fig. 1. Perforated plate, sample C450-0 mounted by means of two steel frames at the basic plate. The scale refers to the perforated plate.

2. Experimental

In this study, perforated plates were made of two types of steel, 50CrV4 and Hardox 450. 50CrV4 was used in accordance to authors previous investigations [11–14], while Hardox 450 was used as a commercial alternative to Armox 450 RHA steel [15,16]. Chemical compositions, tested by ARL-3460 optical emission spectrometer and LECO CS-244 IR spectrometer are given in Table 1.

50CrV4 plates were quenched at 840 °C in oil and subsequently tempered at 170 °C and 450 °C, for achieving two levels of tensile properties, hardness and impact strength. Hardox 450 was used as supplied by the manufacturer. Mechanical properties of these materials were tested at room temperature (20 °C) and are given in Table 2. Tensile properties were obtained In five specimens, by using a tensile testing machine VEB ZDM 5/91 with a maximum tensile force of 49,050 N. Hardness was measured by VEB HPO-250 Brinell and Vickers hardness tester with five indentations on each specimen, while impact strength was measured by Charpy method, by using a WPM 403 tester, in five specimens.

Width and height of all tested plates was 700 × 400 mm, respectively. Their thickness was 6 mm (all tested materials) and 4 mm (only Hardox 450). The holes in perforated plates were machined by water-jet technology, operating at 3500 bar pressure. Perforated plates with two diameters were tested, 7 and 9 mm, with distance between centers of holes 10.5 and 13.5 mm, respectively. Therefore, the ligament between the holes is 3.5 and 4.5 mm, which means that the ratio between hole diameter and the ligament is constant. All perforated plates were placed by means of two steel frames at the maximum distance of 400 mm and 100 mm from the basic 13 mm RHA plate (Fig. 1). This basic RHA plate, at 0° from vertical, protects from 7.92 mm SmK (*Spitzgeschoss mit Kern*) hardened steel core [17].

Various target arrangements were tested, Fig. 2. The first arrangement was to place the perforated plate at 400 mm distance from the basic 13 mm RHA plate, Fig. 2a. The second arrangement had the distance between the perforated and basic plate lowered to 100 mm, Fig. 2b, to investigate if the distance plays a role in separating penetrating core parts in case of fracture. The third arrangement is shown in Fig. 3c and comprised of the perforated plate angled at 20°. The fourth arrangement is similar to the first, the perforated plate placed at 400 mm from the basic plate, but in hanging arrangement, Fig. 2d. The perforated plate was hung by

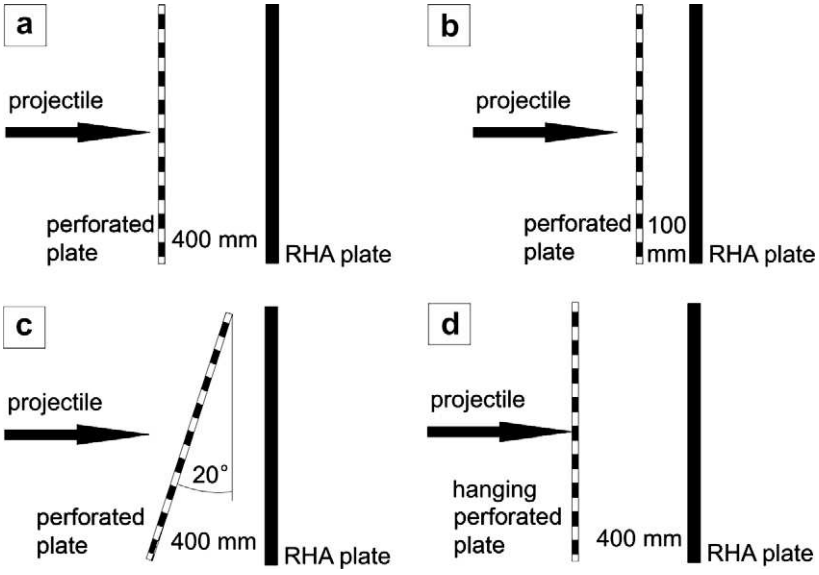

Fig. 2. Test setup of four setups, viewed from above: (a) perforated plate 400 mm from the basic RHA plate, (b) perforated plate 100 mm from the basic RHA plate, (c) perforated plate at 20°, (d) hanging perforated plate at 400 mm from the basic RHA plate.

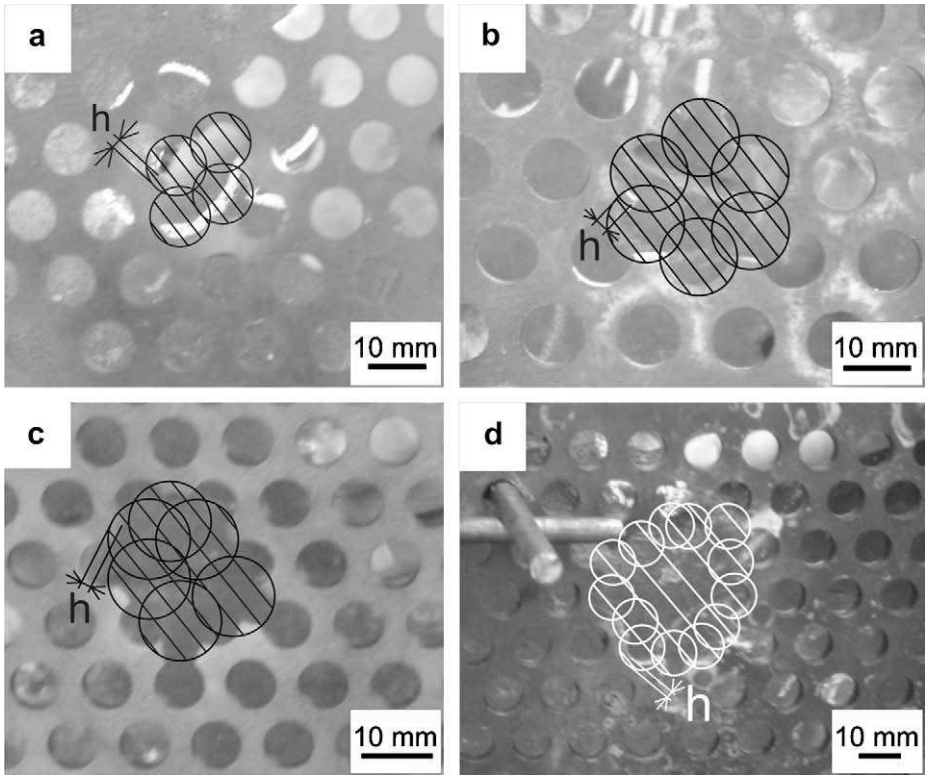

Fig. 3. Representation of damaged area (hatched surface): (a) H9-4-20, shot 2, 4 interconnected holes, (b) H9-4-0, shot 1, 6 interconnected holes, (c) H7-6-0, shot 1, 9 interconnected holes, (d) C170-0, shot 3, 12 interconnected holes.

Table 3
Designation system.

Designation	Target properties				
	Tempering temperature (°C)	Plate thickness (mm)	Hole diameter (mm)	Distance between the perforated and basic plate (mm)	Mounting
C170-0	170	6	9	400	0°[a] inclination
C450-0	450	6	9	400	
C450-20	450	6	9	400	20° inclination
H9-4-0	Used as received from the manufacturer	4	9	400	0°[a] inclination
H9-4-20		4	9	400	20° inclination
H9-4-0H		4	9	400	0°[a] inclination–hanging
H7-4-20		4	7	400	20° inclination
H7-4-0H		4	7	400	0°[a] inclination–hanging
H9-6-0		6	9	400	0°[a] inclination
H9-6-0-100		6	9	100	0°[a] inclination
H7-6-0H		6	7	400	0°[a] inclination–hanging

[a] Perpendicular to the projectile trajectory.

two rings each with a diameter of 100 mm, made of rebar with a wire diameter of 5 mm. These rings were supported by a 25 mm bar, firmly mounted by using two U-shaped hooks, over the frames used for perforated plate mounting in previous tests. Hanging arrangement may serve as a more effective yaw inducer, however, its core fracture potential remains to be found. For more convenience, a designation system for the separate tests in the experiment is presented in Table 3.

Mounting type, angle of incidence and distance between the perforated and the basic plate of the following test were chosen accordingly to the results of previous tests in this paper. Therefore, all mounting types, angles of incidence and distances between the perforated and the basic plate were not tested for all plates.

Ballistic testing was performed by using M-8 API ammunition. This ammunition is used in accordance with the standard procedures described in the 1985 Technical regulations for RHA plate acceptance [17]. Steel core diameter was 10.9 mm, a length of 47.2 mm and a weight of 24.6 g. This ammunition was fired from a Browning M2HB 12.7 × 99 mm heavy machine gun placed on a tripod, from a 100 m distance. For each test, five shots were fired, where penetration criteria was that no projectile penetrates the basic RHA plate (zero penetration criteria) [17].

Perforated plate damage is represented by the area covering the sufficient overlap between the core and the remaining plate. This overlap is 0.34 (h/R, R – core radius), since if it is smaller, the fracture of the core is not assured, as found by Chochron et al. [8]. This is the most unfavourable case, since even if the projectile impacts within the overlap, the stochastic nature of impact may cause the projectile to yaw and impact the basic plate sideways. This way, the penetration of the basic plate is not fully assured, but neverthe-

Table 4
Ballistic testing results.

Target	v_{10} (m/s)	Eq. firing distance (m)	No. of interconnected holes	Damaged area on the perf. plate (mm^2)	Description of basic plate damage, shot No. {[a]}		
					Hole normal	Cracked bulge	Smooth bulge
C170-0	**860.4**	**179**	**7.25** (**5.67**)[b]	**520.18** (**426.06**)[b]	2	5	1,3,4{2}
C450–0	868.9	160	6.33	491.91	1	5{2}	2{2},3{2},4{2}
C450–20	867.8	163	6	447.78	–	2{2}	1{2},3{2},4,5
Average C450			**6.16**	**469.84**			
H7–4-20	868.3	162	6.6	158.39	2–4	1,5	–
H7–4-0H	869.8	158	7.2	190.50	2,3,5	2,4	–
Average H7-4			**6.9**	**174.45**			
H7-6-0	**864.8**	**170**	**9** (**9**)[b]	**274.21** (**286.96**)[b]	1–3,5	–	4{2}
H9-4-0	872.8	152	5.6	436.03	1–3,4	5{2}	–
H9-4-20	877.6	141	5	357.31	1,2,4,5	3{2}	–
H9-4-0H	871.1	155	7.2	576.09	–	1,2,3–5{2}	–
Average H9-4			**5.93**	**456.48**			
H9-6-0	866.9	165	6.4	483.49	–	–	1{4},2,3{3},4{5},6
H9-6-0-100	862.0	176	4.8	255.18	2,3,5	–	1,4
Average H9-6			**5.6**	**385.83**			

[a] Number of *cracks* if crack bulge occured or *core parts* if the core is fractured.
[b] The average results with far from the average results omitted.

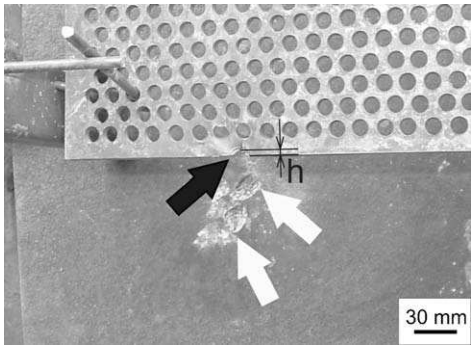

Fig. 4. C450–20 sample with a plate edge impact (black arrow) fracturing the penetrating core in two parts (white arrows). The scale refers to the basic plate.

less possible. Damage area was calculated according to schemes shown in Fig. 3. The schemes were drew in Corel Draw X3 program, saved as a ".dwg" file and then inserted into PTC Pro ENGINEER CAD program. After scaling the scheme to the desired size corresponding to core diameter, the areas were calculated using standard software tools.

BS-850 radar was used to determine muzzle velocity at 10 m from the muzzle, while measured muzzle velocities were compared to the technical regulations for RHA plate acceptance [17]. According to these regulations, muzzle velocity of a M-8 API round fired from a Browning M2HB is 910 ± 15 m/s, or 895–925 m/s. From the measured muzzle velocities, and M2 Browning machine gun Firing Tables Charts [18,19], an equivalent firing distance was found using:

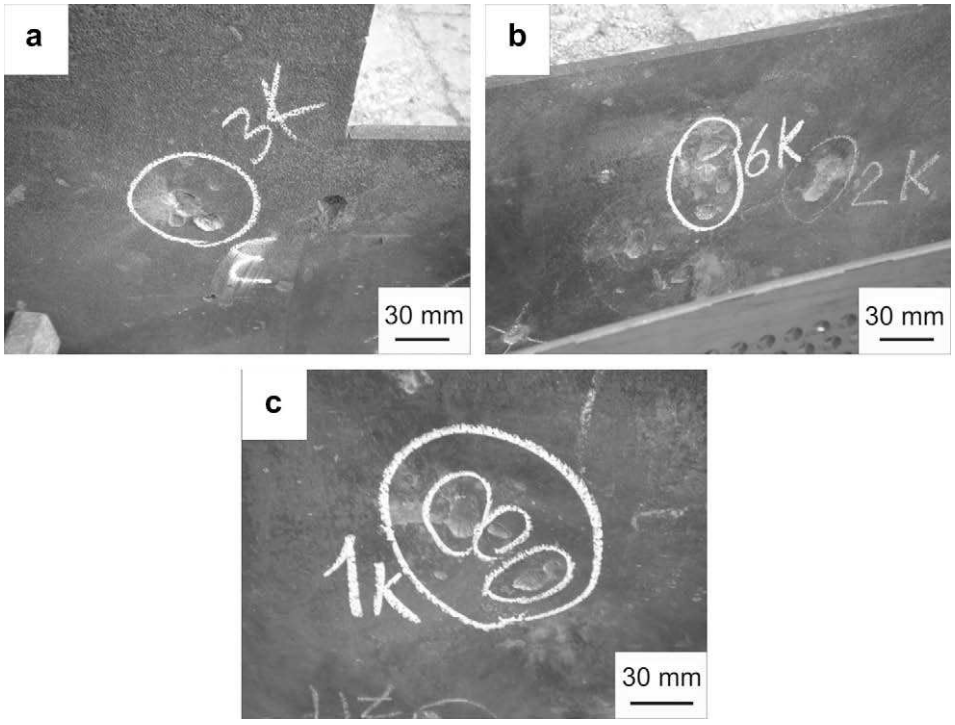

Fig. 5. Penetration core fractured in more than two parts at perforated late sample H9-6-0: (a) shot 3 (three parts), (b) shot 1 (four parts), (c) shot 4 (five parts). Scales refer to the perforated plate.

$$X_e = 100 + X' \quad (1)$$

where, X_e [m] is the equivalent distance, 100 refers to 100 m which is the true firing distance, and X' [m] is the distance that corresponds to the measured muzzle velocity.

The obtained results of basic plate damage on its front and back sides were correlated with perforated plate damage area, as well as the equivalent firing distance.

Fracture surfaces were examined by JEOL JSM-6460LV scanning electron microscope (SEM), operating at 20 kV. Furthermore, energy dispersive X-ray analysis (EDX) was performed, using an Oxford Instruments INCA Microanalysis system.

3. Results

The obtained results are shown in Table 4. It can be seen that muzzle velocities varied considerably, between 847.4 and 891.7 m/s. These values are lower than the range of standard values of 895–925 m/s listed in the 1985 Technical regulations for RHA plate acceptance [17]. Therefore, equivalent firing distances, calculated in accordance to Eq. (1), are given for each shot, calculated according to equation above. Muzzle velocities correspond to equivalent firing distances between 110 and 209 m, Table 4.

Description of basic plate damage was carried out according to STANAG 4146 [20]. In this paper, only three relevant descriptions were found:

1. Hole normal (HN) – a complete hole through the plate of approximately the diameter of the projectile.
2. Cracked bulge (CB) – a bulge on the back of the plate with at least one distinct crack on it.
3. Smooth bulge (SB) – a bulge on the back of the plate without cracks.

However, the description "Smooth bulge" was found to be insufficient in this case, so it was mentioned if the core has been fractured or not, Figs. 4 and 5. If the core fractured, a very important note is the number of parts, since this may influence the damage level found on the basic plate. Core fracture was detected by visual examination of the basic plate, where the number of dents indicates the number of penetrating core pieces.

Damaged area per number of interconnected holes is given in Fig. 6–8. Fig. 6 shows the influence of ductility, on representative samples (C170-0, C450-0 and H9-6-0), Fig. 7 shows the influence of plate thickness (H9-4-0 and H9-6-0), while Fig. 8 shows the influence of hole size (H7-6-0 and H9-6-0).

Fracture surface macro images are shown in Fig. 9. It can be seen that after impact, the back of 50CrV4 perforated plate tempered at 170 °C (shot 4, target C170-0) becomes fractured with the absence of visible plastic deformation, Fig. 9a. On the other hand, significant plastic deformation in impact area of Hardox 450 (shot 5, target H9-6-0) is seen in Fig. 9b. SEM fractographs of 50CrV4 perforated plate tempered at 170 °C (shot 4, target C170-0) and Hardox 450 steel (shot 5, target H9-6-0) are shown in Figs. 10 and 11. Fracture surface of 50CrV4 steel, Fig. 10b and c is mostly smooth and smeared, containing small islands with dimple – like structure. On the other hand, Hardox 450 steel, Fig. 11b and c shows dimples all over the fracture surface. EDX analysis has shown that the fracture surface is covered with debris containing barium, aluminium, copper and magnesium, Fig. 12.

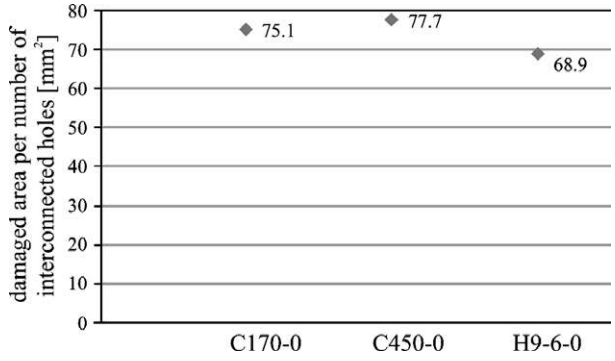

Fig. 6. Damaged area per number of interconnected holes of C170-0, C450-0 and H9-6-0 showing the influence of ductility.

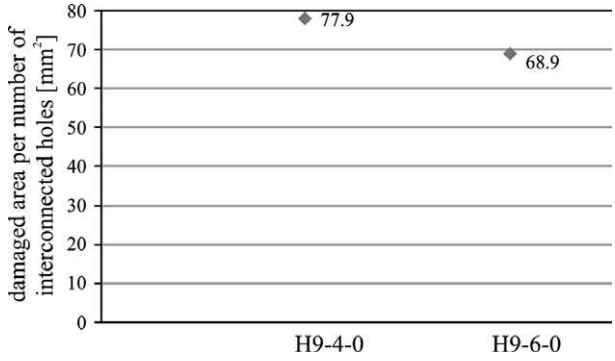

Fig. 7. Damaged area per number of interconnected holes of H9-4-0 and H9-6-0 showing the influence of plate thickness.

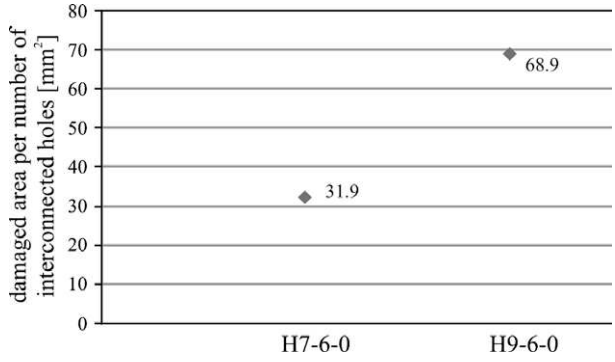

Fig. 8. Damaged area per number of interconnected holes of H7-6-0 and H9-6-0 showing the influence of hole size.

4. Discussion

4.1. Damaged area

As the failure can be somewhat of a stochastic process, even on homogenous plates, on heterogenous types af armour such as perforated plates this nature can only be more pronounced. Therefore, the location of the impact has much to do, along the impact velocity (proportional to muzzle velocity) i.e. impact energy, mechanical properties of the material used, hole size and other factors, with the number of interconnected holes and damaged area on the perforated plate.

Average number of interconnected holes and average damaged area not including impacts on the edges of the perforated plate and impacts on the edges of the already present damaged areas are shown in Table 4. According to these results, influence of hardness, ductility, hole size and plate thickness can be devised, to optimize them to achieve ballistic resistance of the whole package.

Although obviously less important than the effect of the perforated plate on penetration core, that is, ballistic resistance of the

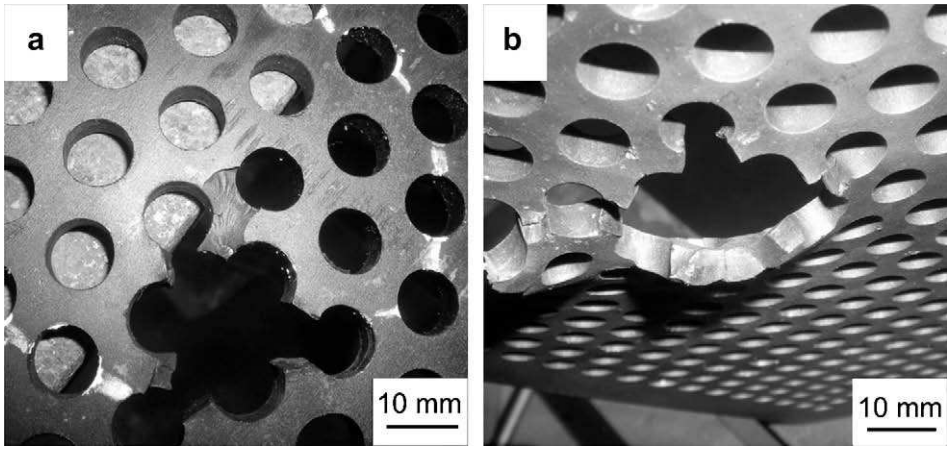

Fig. 9. Fracture surface macro images: (a) 50CrV4 perforated plate tempered at 170 °C (shot 4, target C170-0), (b) Hardox 450 (shot 5, target H9-6-0). Scales refer to the perforated plate in the region of fracture.

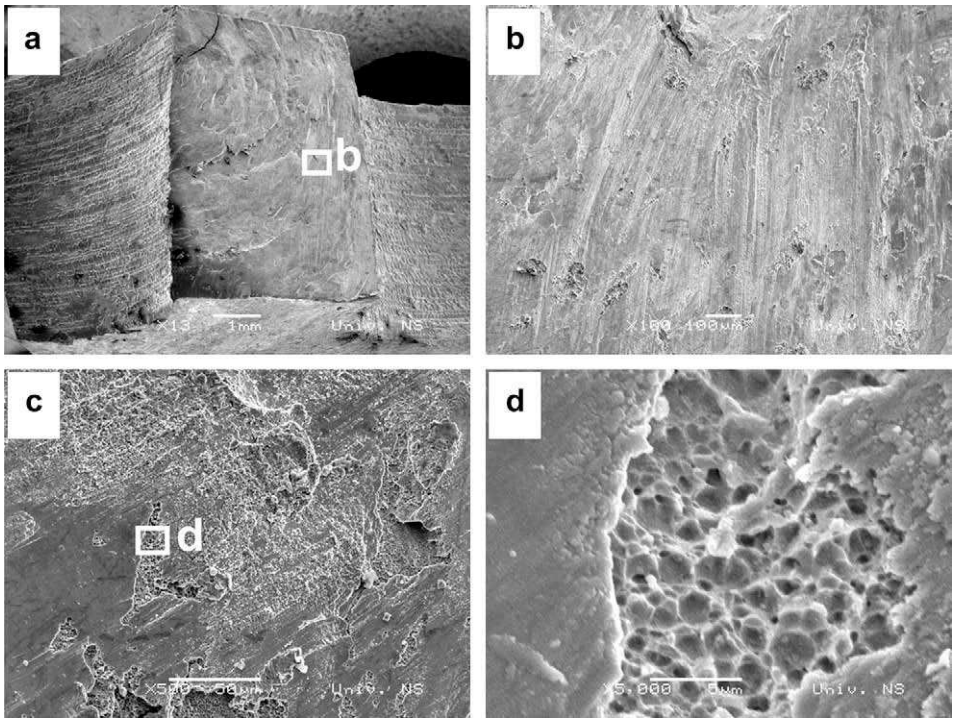

Fig. 10. SEM fractograph of 50CrV4 steel tempered at 170 °C (shot 4, target C170-0): (a) macro image, (b and c) smooth and smeared surface with small islands with dimple – like structure, (d) dimples at a higher magnification.

whole armour model, damaged area may be a decisive factor if two perforated plates offer the same or similar performance.

4.1.1. Hardness and ductility

Hardness and ductility, are inversely proportional for different heat treatment parameters of 50CrV4 steel, Table 2. Therefore, their influence on average number of interconnected holes and average damaged area is different. If the hardness is higher, ultimate tensile stress is higher and the results presented in [8] show a more pronounced effect on the projectile, causing core fracture even on thinner plates. This way, mass efficiency of the armour is increased. On the other hand, harder but less ductile material may suffer from a higher damaged area since plastic deformation does not appear or it is much smaller.

The hardest but least ductile C170-0 has shown to have the highest average number of interconnected holes and therefore the highest average damaged area, if the results which are far from the average are included, Table 4. Therefore, H9-6, which has the same thickness and hole diameter as C170-0 had 35% smaller average damaged area, due to its considerably higher ductility. The influence of ductility may be seen on the example of average damaged area of C450, which is between the values of C170 and H9-6, closely corresponding to its ductility, which is similarly, between ductility values of these two targets. When extreme values are omitted, the average damage areas are similar, however, the difference still exists if damaged area per number of interconnected holes is considered, Fig. 6. Damaged area per number of interconnected holes is higher on less ductile C170 and C450 targets, compared to H9-6-0.

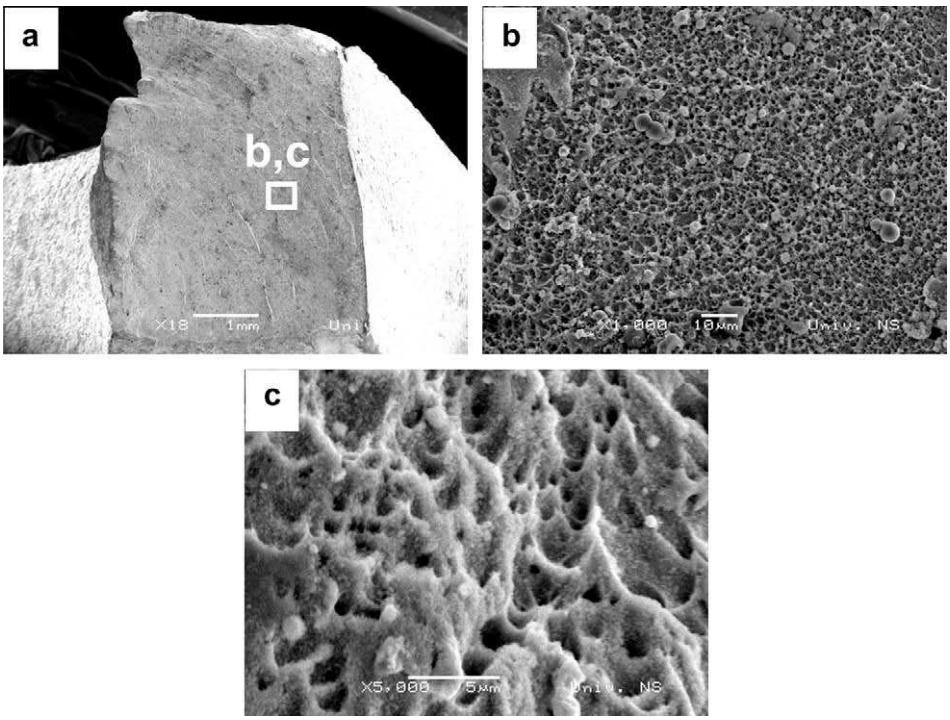

Fig. 11. SEM fractograph of Hardox 450 (shot 5, target H9-6-0): (a) macro image, (b) dimples at 1000×, (c) dimples at 5000×.

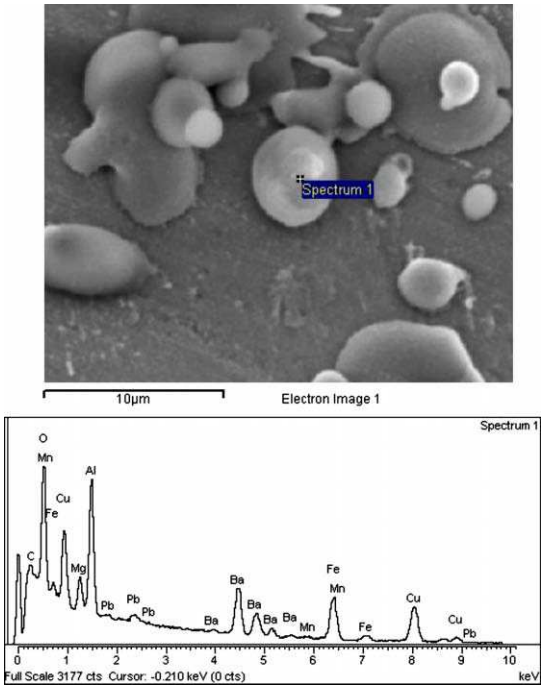

Fig. 12. EDX analysis of debris.

4.1.2. Plate thickness

Plate thickness may have two opposite effects on damaged area. Smaller damaged area may be caused by a higher resistance of a thicker plate. On the other hand, impact energy may cause bending stresses which could be more pronounced if the plate is thicker, causing a larger damaged area.

According to the results shown in Table 4, plate thickness has small, or no effect on damaged area. If targets H9-4 and H9-6 are compared, H9-4 has a larger damaged area. Damaged area per number of interconnected holes is notably higher on thinner targets, as shown in Fig. 7, where H9-6-0 and H9-4-0 targets are compared.

4.1.3. Hole size

Hole size may have two different effects. If the hole diameter/ligament ratio is constant, by decreasing hole size, the ligament becomes smaller too, offering a smaller and less effective obstacle to the incoming projectile, having a lower effect on the projectile. On the other hand, a perforated plate with smaller holes may have a smaller damaged area since the path of the crack propagation may be smaller due to smaller ligament and hole size.

The results shown in Table 4, indicate that smaller holes indeed influence the appearance of a considerably smaller damaged area. If same plate thicknesses are considered, perforated plate with 7 mm hole (H7-6-0) has 54% lower damaged area than the plate with 9 mm hole (H9-6-0), Fig. 8. This indicates that the predominant effect on achieving a lower damaged area is a perforated plate with smaller holes. Furthermore, if plate thickness and ductility are considered, it can be deduced that for a smaller damaged area, it would be beneficial to use a more ductile material, thicker plates and smaller hole size.

4.2. Ballistic resistance

When perforated plate damage in the form of number of interconnected holes or damaged area is compared to basic plate damage, no relationship can be devised. However, there are significant differences of basic plate resistance when various perforated plates are mounted differently, at different angle and distance are compared.

4.2.1. 50CrV4 steel

When a softer, but more ductile perforated plate (C450-0) was mounted at 0°, the damage on the basic plate was similar or slightly lower than when a harder but less ductile plate (C170-0)

Table 5
Targets that offer full protection from 12.7 mm and their properties.

Sample	Cores fractured out of five shots	Damaged area (mm^2)	Areal density of the perforated and basic plate (kg/m^2)	Mass effectiveness of perforated plate	Mass effectiveness of armour model
C450-20	2	469.84	121.8	5.56	1.74
H9-4-0H	0	456.48	114.4	8.88	1.85
H9-6-0	4	385.83	120.6	5.91	1.76

was used, Table 4. This is proved by a more frequent number of core fractures, Fig. 4. Furthermore, more ductile perforated plate damaged area was smaller, so this perforated plate was chosen to be mounted at an angle. When this target was used (C450-20), no penetration of the basic plate was recorded, achieving full ballistic protection according to [17]. Clearly, the slope increases the effectiveness of the perforated plate, since the penetrating core may impact into the hole on the perforated plate by different portions of the *ogival*, which may induce larger yaw.

The first shot is particularly interesting, since the projectile impacted at the edge of the perforated plate, leaving a 2.8 mm deep dent, Fig. 4. When the depth of this dent is divided by the radius of the penetrating core, 2.8/5.45 = 0.51, which supports the results shown in [8].

4.2.2. Hardox 450 steel 7 mm hole

Neither of the tested plate thicknesses offered sufficient protection. It can be noted (Table 4) that the plate with a thickness of 4 mm in hanging arrangement (H7-4-0H) offers a similar or even slightly higher protection than rigidly mounted 6 mm plate (H7-6-0) at 0°. It is clear that by further decreasing of hole diameter, the effectiveness of the perforated plate would fall, making it closer in effectiveness to a homogenous plate, where "edge effect" gradually disappears.

4.2.3. Hadox 450 steel 9 mm hole

From Table 4 it can be seen that the plate with a thickness of 4 mm can not offer sufficient protection of the basic plate unless placed in hanging arrangement. This arrangement has shown to be more effective even than the sloped plate, offering full ballistic protection according to [17]. However, no core fracture has been recorded, indicating that the main mechanism of penetrator defeating is yaw that is induced by the impact into an unhomogenous target. That means a higher damage level on the basic plate – all five of them being "Cracked bulge", of which three with two cracks.

Perforated plate with 6 mm thickness has had the highest effectiveness – almost all penetrating cores were fractured, except the last one, Table 4. When compared to 50CrV4 steel, where penetrating cores were fractured in two parts, perforated plate made of Hardox 450 steel caused the fracture in up to five parts, progressively lowering the damage level of the basic plate, Fig. 5. This way, full ballistic protection was achieved [17]. However, when the distance was lowered to 100 mm, the performance fell considerably. Namely, three "Hole normal" and two "Smooth bulge" plate damage levels were recorded, indicating that even if the core fractures, 100 mm distance is not sufficient to separate the debris enough, spread the kinetic energy and prevent penetration of the basic plate.

4.3. Fracture surfaces

In spite of the absence of visible plastic deformation seen on macro images, Fig. 9, 50CrV4 tempered at 170 °C (the material with the lowest impact strength) has regions with dimples on its fracture surface, a clear indication of ductile fracture (Fig. 10b). The smooth surface present on fracture surface of 50CrV4 is covered by a debris, so its fracture morphology is not clearly identifiable.

The smooth and smeared surface is believed to be caused by the heavy shear deformation of dimples along the direction of shear stress. Higher magnification (Fig. 10d, 5000×) proved that dimples are indeed present on fracture surface, indicating ductile fracture mode, as also has been seen in [20]. According to Fig. 11, fracture mode of Hardox 450 is fully ductile, without smooth and smeared surface area, without catastrophic shear failure.

EDX analysis shown that the surface is covered with debris, containing barium, copper, aluminium and magnesium, Fig. 12. These elements come from the projectile jacket (copper) and incendiary mixture used in M-8 API projectile. Namely, incendiary mixture of API projectile has a designation IM-11 and consists from 50% barium–nitrate $Ba(NO_3)_2$ and 50% magnesium–aluminium alloy [21].

4.4. Mass effectiveness

If samples that offer protection according to regulations (five shots, no penetration) [22] are considered, it can be found that there are three alternatives: C450-20, H9-4-0H and H9-6-0. To find the optimum, their effectiveness in term of cores fractured is considered, as well as their damaged area (regardless of mounting) and mass effectiveness, is shown in Table 5. Mass effectiveness is not calculated taking into consideration perforated plates measured, true mass, but rather theoretical mass, due to small differences in manufacturing process, to avoid inconsistency. Mass efficiency is calculated for the whole package, (basic and perforated plate), with areal density of a 27 mm plate that protects from 12.7 mm M-8 ammunition. According to technical regulations for RHA plate acceptance [22], an RHA plate that offers protection from 12.7 mm M-8 API ammunition fired from a Browning M2HB machine gun has an areal density of 211.9 kg/m^2. From Table 5, it can be seen that H9-4-0H has the highest mass efficiency due to a thinner perforated plate. If only the perforated plate is considered, its mass efficiency is 8.88, which compares favourably with 5.56 and 5.91 for C450-20 and H9-6-0, respectively. However, when the whole armour model is considered (perforated and basic RHA plate), differences are smaller due to a large areal density of the basic plate (102 kg/m^2). Furthermore, H9-6-0 has a smaller damaged area and furthermore, rigid mounting of applique armour is simpler. The highest number of fractured cores and the smallest damage on the basic plate recommend H9-6-0 as the optimal sample. The damage on the basic plate is relatively small, indicating that even a thinner basic plate may be used, further increasing overall mass effectiveness.

5. Conclusions

According to the obtained results, some conclusions can be drawn:

- Steel with a very high hardness and a lower ductility (C170) is not suitable for perforated plates since their damaged area and more importantly, effect on the core is not as pronounced, compared to a steel with more balanced mechanical properties. The

effect of ductility is obvious when medium hardness steel (C450) is compared to Hardox 450, with a similar hardness and lower ductility. C450 is effective only if mounted at an angle. Furthermore, the effect on the penetrating core and mass efficiency are lower than on comparable Hardox 450 perforated plate. The effect of ductility is shown by fracture surfaces, most notably Hardox 450, which does not show catastrophic shear failure.

- Although damaged area is relatively small, perforated plates with hole size of 7 mm are not suitable for defeating 12.7 mm M-8 API ammunition. The main reason is that such perforated plates can not fracture the core often enough. Perforated plates with 9 mm holes and 4 mm thickness are effective yaw inducers only when mounted in a hanging arrangement (H9-4-0H), but do not possess the potential to fracture penetrating cores resulting in a higher basic plate damage. Although mass efficiency is higher than with a thicker 6 mm perforated plate with 9 mm holes (H9-6-0), hanging arrangement is challenging from the point of view of ease of mounting on an actual armoured vehicle.
- The optimal sample has shown to be H9-6-0. Its resistance is sufficient to induce bending stresses in penetrating core to frequently fracture it in more than two parts. Therefore, the debris can not sufficiently affect the basic plate, enabling it to have a very high multi-hit resistance.

Acknowledgement

The authors would like to thank Mr. Jeff Duquette for overall support and useful suggestions in determining a correct terminology of steel RHA steel plate damage.

References

[1] Hazell Paul J, Roberson Colin J, Mauricio Moutinho. The design of mosaic armour: the influence of tile size on ballistic performance. Mater Design 2008;29:1497–503.
[2] Bless SJ, Jurick DL. Design for multi-hit capability. Int J Impact Eng 1998;21:905–8.
[3] de Rosset WS. Patterned armor performance evaluation. Int J Impact Eng 2005;31:1223–34.
[4] Mustafa Übeyli R, Orhan Yıldırım, Bilgehan Ögel. On the comparison of the ballistic performance of steel and laminated composite armors. Mater Design 2007;28:1257–62.
[5] Ogorkiewitz RM. Advances in armour materials. Int Defence Rev 1991;4:349–52.
[6] Ogorkiewitz RM. Armor for light combat vehicles advances in armour materials. Int Defence Rev 2002:41–5.
[7] Marjanovic P. Razvoj oklopa za borbena vozila. Vojnotehnicki Glasnik 1996;1:113–21.
[8] Chocron S, Anderson Jr CE, Grosch DJ, Popelar CH. Impact of the 7 62-mm APM2 projectile against the edge of a metallic target. Int J Impact Eng 2001;25:423–37.
[9] Edwards MR, Mathewson A. The ballistic properties of tool steel as a potential improvised armour plate. Int J Impact Eng 1997;19:297–309.
[10] Borvik T, Dey S, Clausen AH. Perforation resistance of five different high-strength steel plates subjected to small-arms projectiles. Int J Impact Eng 2009;36:948–64.
[11] Balos S. Materials selection and heat treatment technology od steels used for ballistic application. Diploma work, University of Novi Sad, Faculty of Technical Sciences; 2000.
[12] Balos S, Kakas D, Skoric B, Rakita M. The influence of ballistic index on steel selection and armoured vehicle design. In: Proceedings of 2nd design and shaping conference: KOD, 2002, Novi Knezevac, Yugoslavia; 2002. p. 185–190.
[13] Balos S, Sidjanin L, Rajnovic D. Commercial steels as ballistic material. In: Proceedings of 32nd conference on production engineering of Sebia and Montenegro with Foreign participants, Vrnjacka Banja, Serbia and Montenegro; 2005. p. 253–6.
[14] Balos S, Rajnovic D, Sidjanin L. Commercial steels for ballistic application. In: Proceedings of the abstracts CO-MAT-TECH, scientific conference with international participation, Trnava, Slovak Republic; 2004. p. 13.
[15] SSAB Data Sheet, Hardox 450, Swedish steel Oxelösund AB, Sweden; 2007.
[16] SSAB Data Sheet, Armox 450, Swedish steel Oxelösund AB, Sweden; 2007.
[17] SNO 1645 Pancirni lim od celika HPA-10. Technical regulations for RHA plate acceptance; 1985. p. 11.
[18] FT 0.50-H-1 Firing tables. Gun, Machine M2; 1942. p. 51.
[19] War department FM 23-65. Basic Field manual, browning machinegun, Caliber 50 M2, Government Printing Office, Washington, USA; 1940. p. 42.
[20] STANAG 4146. Annex D; 1998. p. D-1.
[21] Liu X, Tan C, Zhang J, Wang F, Cai H. Correlation of adiabatic shearing behavior with fracture in Ti-6Al-4V alloys with different microstructures. Int J Impact Eng 2009;36:1143–9.
[22] SSNO TS I-I/I, M715; 1974. p. 97.